

LETTERS

BAI1 is an engulfment receptor for apoptotic cells upstream of the ELMO/Dock180/Rac module

Daeho Park^{1,2}, Annie-Carole Tosello-Trampont², Michael R. Elliott², Mingjian Lu^{3,†}, Lisa B. Haney², Zhong Ma², Alexander L. Klibanov⁴, James W. Mandell⁵ & Kodi S. Ravichandran^{2,3}

Engulfment and subsequent degradation of apoptotic cells is an essential step that occurs throughout life in all multicellular organisms^{1–3}. ELMO/Dock180/Rac proteins are a conserved signalling module for promoting the internalization of apoptotic cell corpses^{4,5}; ELMO and Dock180 function together as a guanine nucleotide exchange factor (GEF) for the small GTPase Rac, and thereby regulate the phagocyte actin cytoskeleton during engulfment^{4–6}. However, the receptor(s) upstream of the ELMO/Dock180/Rac module are still unknown. Here we identify brain-specific angiogenesis inhibitor 1 (BAI1) as a receptor upstream of ELMO and as a receptor that can bind phosphatidylserine on apoptotic cells. BAI1 is a seven-transmembrane protein belonging to the adhesion-type G-protein-coupled receptor family, with an extended extracellular region^{7–9} and no known ligands. We show that BAI1 functions as an engulfment receptor in both the recognition and subsequent internalization of apoptotic cells. Through multiple lines of investigation, we identify phosphatidylserine, a key ‘eat-me’ signal exposed on apoptotic cells^{10–13}, as a ligand for BAI1. The thrombospondin type 1 repeats within the extracellular region of BAI1 mediate direct binding to phosphatidylserine. As with intracellular signalling, BAI1 forms a trimeric complex with ELMO and Dock180, and functional studies suggest that BAI1 cooperates with ELMO/Dock180/Rac to promote maximal engulfment of apoptotic cells. Last, decreased BAI1 expression or interference with BAI1 function inhibits the engulfment of apoptotic targets *ex vivo* and *in vivo*. Thus, BAI1 is a phosphatidylserine recognition receptor that can directly recruit a Rac–GEF complex to mediate the uptake of apoptotic cells.

Previous studies revealed two ‘functional’ regions within ELMO1 and its *Caenorhabditis elegans* homologue CED-12 during phagocytosis^{5,14–17}. The amino-terminal 558 amino-acid residues (N-term) were necessary for targeting of the ELMO–Dock180 complex to the membrane^{14,17}, whereas the carboxy-terminal 196 residues (C-term) were necessary for binding Dock180 and for optimal Rac activation^{15,16}. Because the receptor(s) upstream of ELMO1 during engulfment were not known, we performed a yeast two-hybrid screen, with N-term as bait. After screening more than 1.1×10^7 colonies from a mouse embryo library, followed by several subscreens for specificity, we identified a single membrane protein, BAI1.

BAI1 belongs to subgroup VII of the adhesion-type G-protein-coupled receptor (GPCR) family^{7–9}, with extended extracellular termini containing multiple domains and motifs that are thought to function in cell–cell or cell–matrix interactions⁹. BAI1 (1,584 residues) has an 943-residue extracellular region, a seven-transmembrane ‘heptahelical body’ and a 392-residue cytoplasmic tail^{7,8} (Fig. 1a). *bail* was initially cloned as a p53-regulated message in the brain⁷ and received its name because an extracellular fragment inhibited

neovascularization in experimental angiogenesis⁷. However, no physiological ligands for BAI1 have been reported. The BAI1 fragment isolated in the two-hybrid screen (residues 1431–1582) was part of its cytoplasmic tail. Yeast transformants expressing BAI1^{1431–1582} and either N-term or full-length ELMO1 (but not C-term) were able to grow under selective conditions (Fig. 1b). Binding of N-term to the cytoplasmic tail of BAI1 or to full-length BAI1 was also confirmed in mammalian cells (Supplementary Fig. 2, and data not shown).

Publicly available gene expression databases indicate the expression of *bail* outside the brain, and microarray analyses also reported *bail* expression in primary human monocytes and macrophages¹⁸. We detected *bail* mRNA and BAI1 protein at different levels in macrophage cell lines (J774 and RAW264.7) and primary tissues such as bone marrow and spleen (Fig. 1c and Supplementary Fig. 1). As reported previously^{7,8}, endogenous BAI1 migrated at the predicted

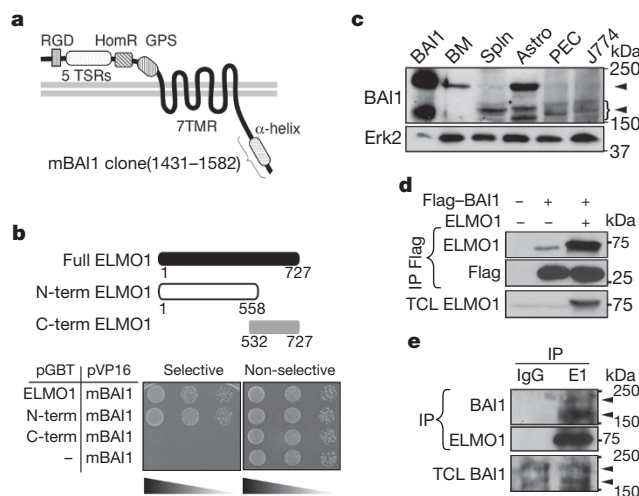


Figure 1 | Identification of BAI1 as an ELMO1-interacting protein.

a, Diagram of BAI1. RGD, integrin-binding motif; HomR, hormone receptor; GPS, GPCR proteolytic site; 7TMR, seven-transmembrane receptor. **b**, A BAI1 clone was tested for interaction with the indicated ELMO1 constructs for growth on selective plates at tenfold dilutions. **c**, Immunoblotting for BAI1 expression shows a 160–170-kDa lower band (often a doublet) and a 220-kDa upper band^{7,8}. BM, bone marrow; Spln, spleen; Astro, astrocytes; PEC, peritoneal exudate cells. **d**, Flag–BAI1 was transfected into LR73 cells, and simultaneous precipitation of endogenous ELMO1 (or transfected ELMO1; lane 3) was determined by anti-ELMO1 immunoblotting. IP, immunoprecipitation. TCL, total cell lysates. **e**, Mouse brain lysates were immunoprecipitated with ELMO1 antibody and simultaneous precipitation of endogenous BAI1 (arrowheads), assessed by immunoblotting. E1, ELMO1.

¹Department of Cell Biology, ²Carter Immunology Center, ³Department of Microbiology, ⁴Cardiovascular Division and ⁵Department of Pathology, University of Virginia, Charlottesville, Virginia 22908, USA. †Present address: Institute for Diabetes, Obesity and Metabolism, University of Pennsylvania School of Medicine, Philadelphia, Pennsylvania 19104, USA.

160–170 kDa (often as a doublet) and an upper 220-kDa band, with various intensities in different cell types (Fig. 1c). Endogenous ELMO1 precipitated together with overexpressed Flag-tagged BAI1, and association at native levels was also confirmed by co-precipitation of endogenous ELMO1 and BAI1 from mouse brain lysates (Fig. 1d, e).

We confirmed that an N-terminally haemagglutinin (HA)-tagged BAI1 (with the tag inserted after the leader sequence) was detectable on the cell surface by flow cytometry (Fig. 2a). Untagged BAI1 was also present in the membrane fractions (Supplementary Fig. 3). To address the role of BAI1 as an engulfment receptor, we generated J774 macrophage cells stably expressing the HA-tagged BAI1. In engulfment assays based on flow cytometry, expression of BAI1 enhanced the uptake of apoptotic thymocytes compared with controls (a fold increase of 2.61 ± 0.11 (mean \pm s.d.), $P < 0.0001$, $n = 7$; Fig. 2b). The increased uptake by BAI1-expressing J774 cells occurred more towards apoptotic cells than towards necrotic and live cells (Fig. 2b). LR73 fibroblasts transiently transfected with BAI1 carrying different tags also enhanced the engulfment of apoptotic thymocytes (Supplementary Fig. 4) or fluorescently labelled 2- μ m carboxylate-modified beads, surrogate targets that mimic apoptotic cells^{19,20} (a fold increase of 2.62 ± 0.20 for green fluorescent protein (GFP)-labelled BAI1, $P < 0.001$, $n = 16$; Fig. 2c). Thus, the BAI1-dependent increased uptake occurred in both macrophages and non-professional phagocytes, with the effect being independent of the tag added. BAI1 lacking either the cytoplasmic or extracellular regions showed no such enhanced uptake, indicating a requirement for both regions (Fig. 2d). Expression of the BAI1 cytoplasmic region alone, capable of binding ELMO1, also had a minimal effect on engulfment over the control (Fig. 2d).

We then tested whether BAI1 promoted engulfment by enhanced binding of targets, by internalization, or by both methods. First, BAI1-GFP-transfected cells showed increased binding of targets (Fig. 2e); second, BAI1-expressing cells ingesting targets had a higher

mean fluorescence intensity (MFI) (where MFI reflects the target-derived fluorescence per cell⁴; Fig. 2b, c). When we quantified the efficiency of internalization (with Amnis ImageStream²¹, which combines flow cytometry with imaging of individual cells), BAI1-GFP-expressing cells exhibited enhanced engulfment, with two or more targets per phagocyte (40% versus 16% in the control; Fig. 2e). Moreover, only BAI1-GFP cells had four or five targets per phagocyte (Fig. 2e). BAI1-GFP was enriched at the phagocytic cup and its localization was correlated with polymerized actin at the same site, as determined by confocal microscopy (Fig. 2f). Thus, BAI1 contributes to both the binding and the engulfment of targets.

BAI1 contains five thrombospondin type 1 repeats (TSRs) in its extracellular region (Fig. 1a). Because TSRs can bind phosphatidylserine (PtdSer)²², we examined whether the TSRs of BAI1 participated in target recognition. Several lines of evidence collectively suggested a role for the TSRs of BAI1 in direct PtdSer recognition and in promoting the engulfment of apoptotic targets. First, the addition of annexin V, which binds PtdSer exposed on apoptotic cells, inhibited BAI1-mediated uptake in a dose-dependent manner (Fig. 3a). We then generated bacterial constructs with or without the TSRs (denoted RGD-TSR or RGD- Δ TSR, respectively; Fig. 3b). The addition of bacterially purified RGD-TSR protein inhibited BAI1-dependent uptake in a dose-dependent manner, whereas glutathione S-transferase (GST) alone or RGD- Δ TSR did not (Fig. 3c and Supplementary Fig. 5). Because the extracellular region of BAI1 also contains an RGD motif, which could potentially participate in integrin-dependent phagocyte-target interactions, we tested proteins with mutations in the RGD motif (RGE-TSR; Fig. 3b). RGE-TSR still inhibited uptake, but deletion of the TSRs (RGE- Δ TSR) abrogated the inhibition (Fig. 3c). The RGD motif in BAI1 was therefore dispensable for engulfment under these conditions, whereas the TSRs were essential.

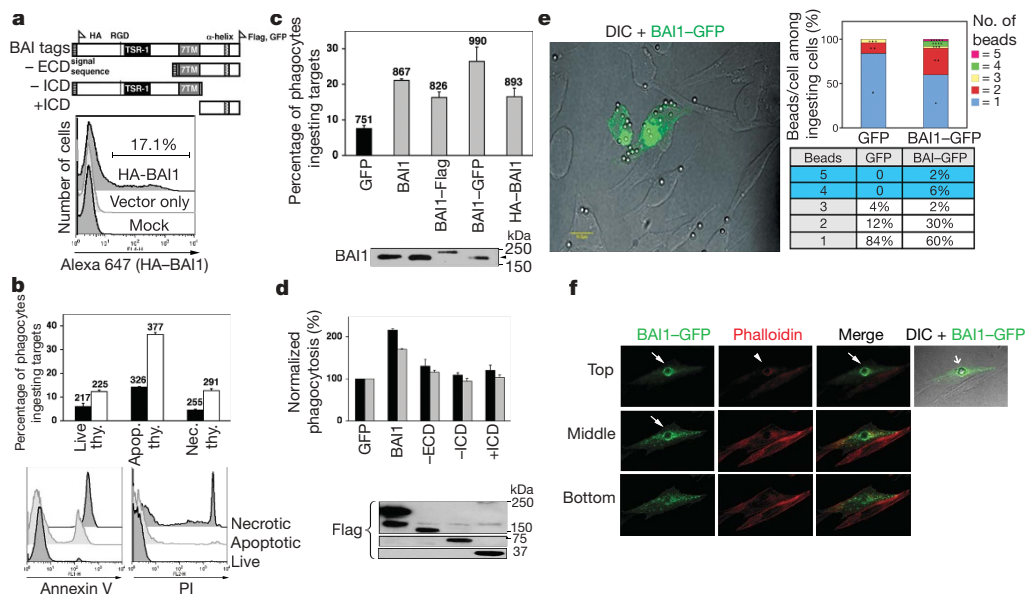


Figure 2 | BAI1 enhances uptake of apoptotic targets. **a**, Top: diagram of BAI1 plasmid constructs used. Bottom: N-terminally HA-tagged BAI1 on the cell surface of transfected LR73 cells was assessed by flow cytometry with anti-HA antibody. ECD, extracellular domain; ICD, intracellular domain. **b**, J774 macrophage cells stably transfected with BAI1 (open columns) or control vector (filled columns) were incubated with live, necrotic or apoptotic thymocytes (thy.) and assessed for enhanced uptake. The numbers above the bars refer to MFI, indicative of target-derived fluorescence per phagocyte. **c**, LR73 cells were transiently transfected with tagged or untagged BAI1, and the uptake of 2- μ m carboxylate-modified beads or apoptotic thymocytes was assessed by a flow-cytometry-based engulfment assay (with MFI of cells ingesting targets shown). Expression of the transfected proteins was confirmed. **d**, BAI1 lacking the intracellular domain (ICD) or

extracellular domain (ECD) regions, or the ICD alone were tested in LR73 cells for BAI1-mediated increased uptake of apoptotic thymocytes (grey columns) and surrogate targets (black columns). **e**, Left: BAI1-GFP-expressing LR73 cells were incubated with unlabelled 2- μ m carboxylate beads; the enhanced binding of targets expressing BAI1-GFP is shown. DIC, differential interference contrast. Right: using Amnis Image Stream, the number of targets within the GFP-expressing or BAI1-GFP-expressing cells were counted and plotted. **f**, BAI1-GFP-expressing LR73 cells were incubated with 6- μ m carboxylate beads and stained with phalloidin; images from different confocal planes are shown to indicate the localization of BAI1-GFP to the phagocytic cup. BAI1 (arrow) and actin (arrowhead) are indicated. Error bars indicate s.d.

When we tested the direct binding of bacterially purified TSRs to apoptotic cells, RGD-TSR could decorate the surfaces of apoptotic cells, in a comparable manner to annexin V staining (Fig. 3d). In competition experiments, unlabelled soluble BAI1-TSR (but not those lacking the TSRs) inhibited the binding of fluorescent annexin V to surrogate targets (Fig. 3e) and apoptotic cells (Supplementary Fig. 6). Furthermore, LR73 cells expressing BAI1-GFP showed enhanced uptake of synthetic 2- μ m microbubbles containing phosphatidylserine (15% PtdSer and 85% phosphatidylcholine; Fig. 3g), with negligible uptake of phosphatidylcholine microbubbles.

Purified proteins with BAI1-TSRs also bound to membrane strips spotted with various phospholipids (Fig. 3h). Under these conditions, the TSRs also showed binding to cardiolipin (a mitochondrial lipid), as well as weaker binding to phosphatidic acid and PtdIns(4)P, but not to other negatively charged lipids on the membrane (Fig. 3h). The binding to sulphatide served as a positive control²³. This suggested a direct interaction between BAI1-TSRs and PtdSer in the absence of other cellular proteins. PtdSer recognition through

BAI1 seemed stereospecific, because the addition of phospho-L-serine, but not phospho-D-serine, strongly inhibited the BAI1-dependent enhanced uptake of apoptotic cells (Fig. 3i). Taken together, the above data showed BAI1 to be a new type of PtdSer-recognition receptor and implicated the TSRs of BAI1 in the direct interaction with phosphatidylserine.

We next addressed the requirement for ELMO1 binding to BAI1 in mediating signalling to promote engulfment. We first narrowed the ELMO1 binding to a short α -helical stretch within the BAI1 cytoplasmic tail, which was necessary and sufficient (Supplementary Fig. 7). Mutation of three positive charges within this α -helix (RKR \rightarrow AAA) reproducibly reduced the binding of ELMO1 to BAI1 (Fig. 4a). Full-length BAI1 with this mutation failed to promote enhanced engulfment of apoptotic thymocytes (Fig. 4b). To test the role of ELMO1 in BAI1-mediated uptake directly, we performed stable knockdown of ELMO1 in J774 macrophages with short hairpin RNA (shRNA) targeted to *elmo1*. Transient expression of BAI1 promoted engulfment of apoptotic thymocytes in control shRNA cells but not in cells with ELMO1 knockdown (Fig. 4c). This suggested a requirement for ELMO1 expression for enhanced engulfment mediated by BAI1.

BAI1 formed a complex with Dock180, but this association was indirect because it required an interaction of BAI1 with ELMO1 (Fig. 4d). Guanine nucleotide exchange activity towards Rac was detectable in BAI1 precipitates when expressed with ELMO and Dock180 (data not shown). We then asked whether BAI1 expression would alter the levels of activated Rac (Rac-GTP) during phagocytosis. The basal level of Rac-GTP in BAI1-transfected LR73 cells was comparable to that in the mock-transfected cells. However, BAI1-expressing cells showed greater Rac-GTP after addition of targets (30 min), with the Rac-GTP levels returning to the basal state at later time points (Fig. 4e). These data suggested an inducible and transient Rac activation due to BAI1 during the recognition and engulfment of targets.

Whereas overexpression of BAI1 alone or of Dock180/ELMO proteins in LR73 cells increased engulfment, expression of all three proteins simultaneously caused the greatest increase in uptake of both apoptotic thymocytes and surrogate targets (Fig. 4f). This enhancement was lost when a mutant Dock180 (Dock-ISP)⁵ that cannot activate Rac was expressed at the same time, and also resulted in inhibition of the uptake due to BAI1. Similarly, a mutant form of ELMO1 (T625) that can bind BAI1 but cannot link to Dock180 (ref. 5) also failed to promote uptake (Fig. 4f). Last, a dominant-negative

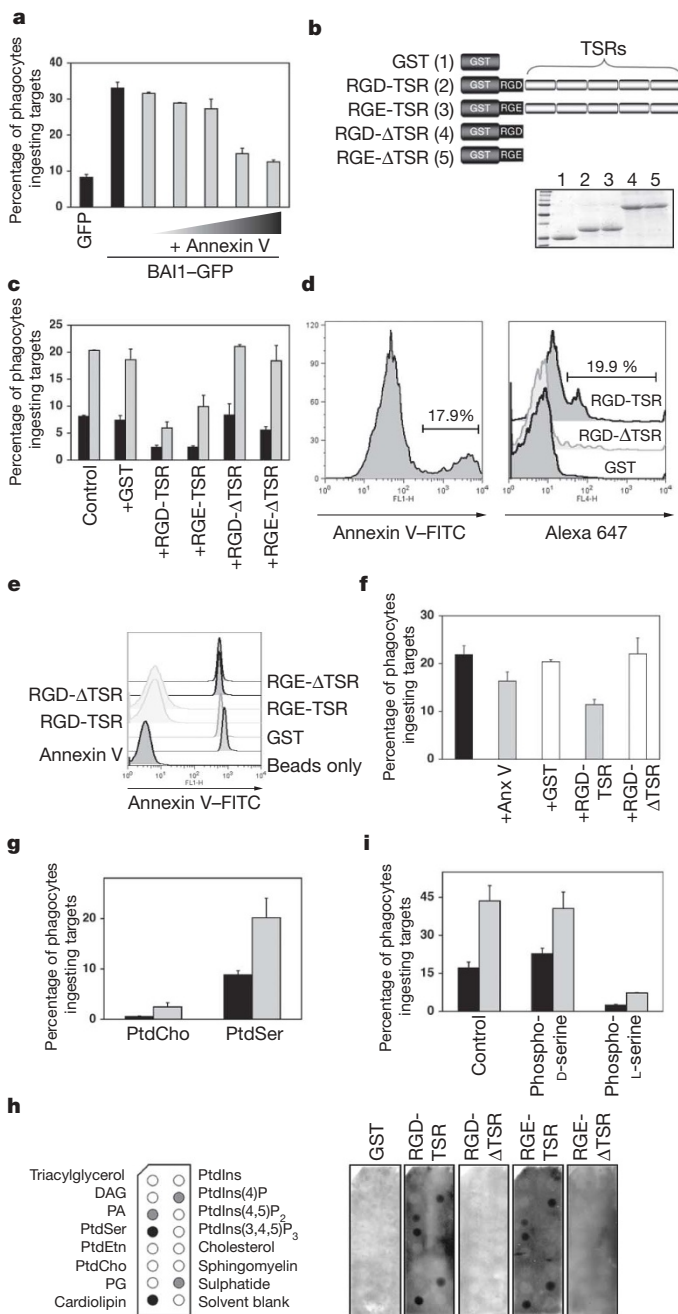


Figure 3 | Recognition of phosphatidylserine by TSRs. **a**, LR73 cells transfected with BAI1 were tested for engulfment of 2- μ m carboxylate beads in the presence or absence of annexin V (0.01–10 μ g μ l⁻¹). **b**, Schematic diagram of constructs containing the TSRs and/or RGD motifs, and Coomassie staining of purified proteins. **c**, Addition of soluble RGD-TSR (10 μ g μ l⁻¹), but not GST or Δ TSR, blocked BAI1-mediated enhanced uptake in LR73 cells. Black columns, GFP; grey columns, BAI1. **d**, Apoptotic Jurkat cells were incubated with indicated soluble BAI1 fragments and their binding was assessed by flow cytometry. Binding of annexin V to the same apoptotic cells is shown for comparison. FITC, fluorescein isothiocyanate. **e**, Soluble RGD-TSR, RGE-TSR, RGD- Δ TSR and RGE- Δ TSR (2 μ g μ l⁻¹ each) were tested for blocking the binding of annexin V to carboxylate-modified beads by flow cytometry. **f**, Uptake of apoptotic thymocytes by J774 cells was tested in the presence of the indicated proteins (10 μ g μ l⁻¹ each). Anx, annexin. **g**, LR73 cells transfected with BAI1-GFP (grey columns) or control GFP alone (black columns) were tested for uptake of phosphatidylserine (PtdSer)-containing microbubbles or the control phosphatidylcholine (PtdCho) bubbles. **h**, Direct binding of soluble BAI1 proteins to phosphatidylserine and other phospholipids spotted on nitrocellulose membrane strips. DAG, diacylglycerol; PtdEtn, phosphatidylethanolamine. PA, phosphatidic acid, PG, phosphatidylglycerol. **i**, Stereospecificity of PtdSer recognition through BAI1-TSRs was tested by the addition of phospho-L-serine or phospho-D-serine during uptake of apoptotic thymocytes by control (black columns) or BAI1-overexpressing (grey columns) J774 cells. Error bars indicate s.d.

mutant of Rac (Rac^{T17N}) also inhibited the uptake mediated by BAI1 (Fig. 4f). The augmented uptake due to simultaneous expression of BAI1, ELMO1 and Dock180 was due to the internalization of targets rather than to enhanced binding (not shown). Taken together, these data suggest that the intracellular tail of BAI1 mediates signalling through the ELMO/Dock180/Rac module to promote the engulfment of apoptotic cells.

Previous studies have suggested redundancy among engulfment receptors expressed on the surface of phagocytes. To test the relative importance for BAI1-mediated engulfment, we performed three types of analysis. First, short interfering RNA (siRNA)-mediated knockdown of BAI1 in primary mouse astrocytes resulted in a decreased uptake of apoptotic thymocytes or carboxylate beads (Fig. 4g). The efficiency of BAI1 knockdown (46%) was approximately correlated with the observed roughly 50% inhibition of engulfment. In J774 macrophages we could achieve only minimal knockdown of BAI1, but this was commensurate with a modest decrease in engulfment (Supplementary Fig. 8). The addition of soluble BAI1 TSRs with apoptotic thymocytes or carboxylate beads also blocked the engulfment of apoptotic cells by J774 cells (Fig. 3f) and primary mouse astrocytes (Fig. 4h). This suggested that BAI1-mediated recognition, under native conditions, does contribute to engulfment in macrophages.

To test the potential importance of BAI1-TSR-dependent recognition *in vivo*, we injected red-fluorescent-labelled carboxylate beads

or apoptotic thymocytes into the peritoneum of mice, with or without simultaneous injection of a soluble BAI1-TSR fragment or GST. After 20 min, we collected the peritoneal lavage cells and determined the fraction of F4/80-positive macrophages with engulfed targets. Simultaneous injection of BAI1-TSRs, but not that of GST, strongly inhibited the ability of peritoneal macrophages to engulf carboxylate-modified beads (Fig. 4i) or apoptotic thymocytes (Fig. 4j and Supplementary Fig. 9). These data further support a role for BAI1 as an engulfment receptor in this *in vivo* model of engulfment.

Taken together, our data yield the following observations. Over the years, the receptor(s) that can directly engage PtdSer and how they may signal intracellularly have remained elusive. This work reveals BAI1 as one type of engulfment receptor that can stereospecifically engage PtdSer on apoptotic cells (through its TSRs). Our work also identifies a receptor upstream of the ELMO/Dock180/Rac signalling module, which has also remained unknown. This could be of great help in defining molecular events from PtdSer-dependent apoptotic cell recognition to responses within the phagocyte¹². BAI1 is also a new type of engulfment receptor belonging to the adhesion-type GPCR family. Treatment of BAI1-transfected cells with pertussis toxin did not affect the enhanced uptake through BAI1, but BAI1 with gross deletion of the seven-transmembrane region failed to promote engulfment (data not shown). Thus, the specific role of the seven-transmembrane region of BAI1 remains to be determined.

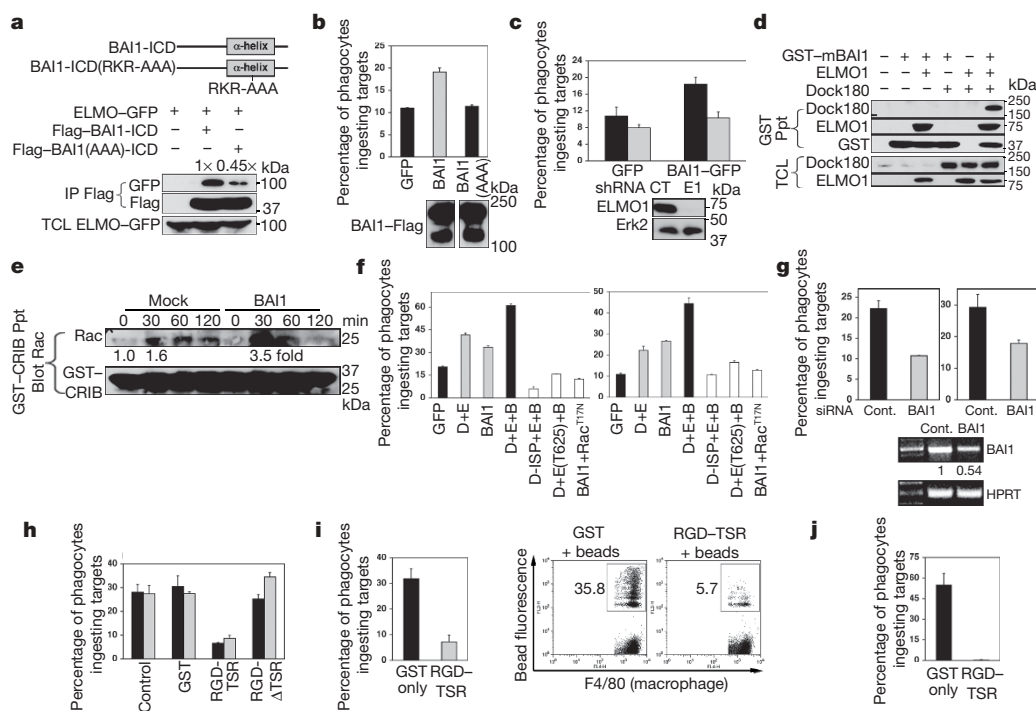


Figure 4 | BAI1 functions upstream of the ELMO/Dock180/Rac module.

a, Top: diagram of the cytoplasmic tail of BAI1 and the RKR→AAA mutation. Binding of this BAI1 mutant to ELMO1 was assessed (relative densitometry signals for ELMO1 are indicated). **b**, Full-length BAI1 with the RKR→AAA mutation fails to enhance uptake of apoptotic thymocytes in LR73 cells. **c**, Top: control shRNA (black columns) or ELMO1 knockdown J774 cells (grey columns) were transfected with either BAI1-GFP or GFP alone, and the uptake of apoptotic thymocytes was assessed. Bottom: knockdown of ELMO1. **d**, 293T cells were transfected with the indicated combination of BAI1, ELMO1 and Dock180 plasmids, and complex formation was determined by immunoblotting. Ppt, precipitation. **e**, Top: Rac-GTP levels after incubation of targets with BAI1-expressing cells or controls. Bottom: densitometry for Rac-GTP signal and comparable GST-CRIB domain in the different lanes are shown. **f**, Engulfment of apoptotic thymocytes (left) or 2- μ m carboxylate beads (right) by LR73 cells transfected with BAI1-GFP (B) and the indicated combinations of ELMO1 (E), Dock180 (D), and the dominant-negative forms of ELMO1 (ET625),

Dock180 (D-ISP) or Rac (Rac^{T17N}). Protein expression of the transfected plasmids was confirmed (data not shown). **g**, Top: knockdown of BAI1 in primary mouse astrocytes inhibits engulfment of apoptotic thymocytes (left) and surrogate targets (right). Bottom: the knockdown, as determined by *bai1* expression or control (cont.) hypoxanthine-guanine phosphoribosyltransferase (HPRT) message, and the efficiency of knockdown. **h**, Engulfment of apoptotic thymocytes (grey columns) or carboxylate beads (black columns) by primary astrocytes was assessed in the presence of the indicated soluble BAI1 proteins or GST alone ($10 \text{ ng } \mu\text{l}^{-1}$ each). **i**, BAI1 TSR repeats or GST were injected together with red-labelled carboxylate beads into the peritoneum of C57/Bl6 mice (three mice per condition, two independent experiments). After 20 min, the fraction of F4/80-positive peritoneal macrophages ingesting targets was assessed (left) and a representative flow cytometry panel is also shown (right). **j**, As in **i**, except that *LysM-Cre/YFP* mice were used and the uptake of apoptotic thymocytes by YFP-positive cells (98% being F4/80-positive) was assessed. Error bars indicate s.d.

Last, the loss of BAI1 from gliomas seems to promote the formation of more aggressive glioblastomas^{7,8}; conversely, overexpression of BAI1 inhibits the neo-vascularization of gliomas and inhibits tumour formation²⁴. Because the natural function of BAI1 in tissues is not known, its identification as an engulfment receptor upstream of the ELMO/Dock180/Rac module could have implications for the treatment of glioblastomas.

METHODS SUMMARY

General. Immortalized cell lines and primary cells were maintained as described previously⁵. All DNA constructs were generated by PCR-based methodology, with the fidelity and presence of appropriate mutations being confirmed by sequencing. The HF7C yeast strain (with His, Trp and Leu as selection markers)²⁵ was used for the yeast two-hybrid screen against a mouse embryo library. Immunoprecipitation and GST pull-down assays were used to detect protein–protein interactions²⁰. Protein expressions and the presence of bound proteins were confirmed by western blotting. Transiently transfected siRNA and stably expressed shRNA were used to knock down the level of BAI1 or ELMO1 proteins. RT–PCR was used to detect the level of mRNA of a specific gene.

In vitro phagocytosis assay. Various cell lines (LR73 Chinese hamster ovary cells, J774 macrophages and NIH 3T3 cells) and primary cells (mouse astrocytes) were transiently or stably transfected before the phagocytosis assays²⁰. Phagocytic cells were incubated with fluorescently labelled targets such as apoptotic thymocytes, 2- μ m carboxylate-modified latex beads, or 2- μ m phospholipid containing microbubbles. After 2 h, the cells were extensively washed with cold PBS, treated with trypsin and resuspended in cold medium containing 1% NaN₃, and analysed by flow cytometry as described previously²⁰.

In vivo engulfment assay. Surrogate beads or apoptotic thymocytes stained with 5- (and 6)-carboxytetramethylrhodamine (TAMRA) were mixed with soluble GST or RGD-TSR protein. The mixture was then injected into the peritoneum of either wild-type C57/Bl6 mice or a LysM-Cre/yellow fluorescent protein (YFP) reporter mouse line (in which 98% of YFP-positive cells in the peritoneum were also F4/80 positive). Peritoneal exudate cells were collected and either F4/80-positive or YFP-positive cells were gated and fluorescence-activated cell sorting analyses were performed to determine the effects of soluble proteins on phagocytosis *in vivo*.

Full Methods and any associated references are available in the online version of the paper at www.nature.com/nature.

Received 26 July; accepted 1 October 2007.

Published online 24 October 2007.

- Savill, J., Dransfield, I., Gregory, C. & Haslett, C. A blast from the past: clearance of apoptotic cells regulates immune responses. *Nature Rev. Immunol.* **2**, 965–975 (2002).
- Henson, P. M. Engulfment: ingestion and migration with Rac, Rho and TRIO. *Curr. Biol.* **15**, R29–R30 (2005).
- Gregory, C. D. & Brown, S. B. Apoptosis: eating sensibly. *Nature Cell Biol.* **7**, 1161–1163 (2005).
- Gumienny, T. L. *et al.* CED-12/ELMO, a novel member of the crkl/Dock180/Rac pathway, is required for phagocytosis and cell migration. *Cell* **107**, 27–41 (2001).
- Brugnera, E. *et al.* Unconventional Rac-GEF activity is mediated through the Dock180-ELMO complex. *Nature Cell Biol.* **4**, 574–582 (2002).
- Lu, M. & Ravichandran, K. S. Dock180-ELMO cooperation in Rac activation. *Methods Enzymol.* **406**, 388–402 (2006).
- Nishimori, H. *et al.* A novel brain-specific p53-target gene, BAI1, containing thrombospondin type 1 repeats inhibits experimental angiogenesis. *Oncogene* **15**, 2145–2150 (1997).
- Kaur, B., Brat, D. J., Devi, N. S. & Van Meir, E. G. Vasculostatin, a proteolytic fragment of brain angiogenesis inhibitor 1, is an antiangiogenic and antitumorigenic factor. *Oncogene* **24**, 3632–3642 (2005).
- Bjarnadottir, T. K. *et al.* The human and mouse repertoire of the adhesion family of G-protein-coupled receptors. *Genomics* **84**, 23–33 (2004).

- Fadok, V. A. *et al.* Exposure of phosphatidylserine on the surface of apoptotic lymphocytes triggers specific recognition and removal by macrophages. *J. Immunol.* **148**, 2207–2216 (1992).
- Henson, P. M. & Hume, D. A. Apoptotic cell removal in development and tissue homeostasis. *Trends Immunol.* **27**, 244–250 (2006).
- Kiss, R. S., Elliott, M. R., Ma, Z., Marcel, Y. L. & Ravichandran, K. S. Apoptotic cells induce a phosphatidylserine-dependent homeostatic response from phagocytes. *Curr. Biol.* **16**, 2252–2258 (2006).
- Wu, Y., Tibrewal, N. & Birge, R. B. Phosphatidylserine recognition by phagocytes: a view to a kill. *Trends Cell Biol.* **16**, 189–197 (2006).
- Grimsley, C. M. *et al.* Dock180 and ELMO1 proteins cooperate to promote evolutionarily conserved Rac-dependent cell migration. *J. Biol. Chem.* **279**, 6087–6097 (2004).
- Lu, M. *et al.* PH domain of ELMO functions in trans to regulate Rac activation via Dock180. *Nat. Struct. Mol. Biol.* **11**, 756–762 (2004).
- Lu, M. *et al.* A steric-inhibition model for regulation of nucleotide exchange via the Dock180 family of GEFs. *Curr. Biol.* **15**, 371–377 (2005).
- deBakker, C. D. *et al.* Phagocytosis of apoptotic cells is regulated by a UNC-73/TRIO-MIG-2/RhoG signaling module and armadillo repeats of CED-12/ELMO. *Curr. Biol.* **14**, 2208–2216 (2004).
- Cho, H. *et al.* Induction of dendritic cell-like phenotype in macrophages during foam cell formation. *Physiol. Genomics* **29**, 149–160 (2007).
- Erwig, L. P. *et al.* Differential regulation of phagosome maturation in macrophages and dendritic cells mediated by Rho GTPases and ezrin-radixin-moesin (ERM) proteins. *Proc. Natl Acad. Sci. USA* **103**, 12825–12830 (2006).
- Tosello-Trampont, A. C. *et al.* Identification of two signaling submodules within the Crkl/ELMO/Dock180 pathway regulating engulfment of apoptotic cells. *Cell Death Differ.* **14**, 963–972 (2007).
- Adang, L. A., Parsons, C. H. & Kedes, D. H. Asynchronous progression through the lytic cascade and variations in intracellular viral loads revealed by high-throughput single-cell analysis of Kaposi's sarcoma-associated herpesvirus infection. *J. Virol.* **80**, 10073–10082 (2006).
- Manodori, A. B., Barabino, G. A., Lubin, B. H. & Kuypers, F. A. Adherence of phosphatidylserine-exposing erythrocytes to endothelial matrix thrombospondin. *Blood* **95**, 1293–1300 (2000).
- Guo, N. H. *et al.* Heparin- and sulfatide-binding peptides from the type I repeats of human thrombospondin promote melanoma cell adhesion. *Proc. Natl Acad. Sci. USA* **89**, 3040–3044 (1992).
- Kang, X. *et al.* Antiangiogenic activity of BAI1 *in vivo*: implications for gene therapy of human glioblastomas. *Cancer Gene Ther.* **13**, 385–392 (2006).
- Lindsay, M. E., Holaska, J. M., Welch, K., Paschal, B. M. & Macara, I. G. Ran-binding protein 3 is a cofactor for Crm1-mediated nuclear protein export. *J. Cell Biol.* **153**, 1391–1402 (2001).

Supplementary Information is linked to the online version of the paper at www.nature.com/nature.

Acknowledgements We thank J. Casanova, C. Grimsley and members of the Ravichandran laboratory for suggestions and for critical reading of the manuscript. This work was supported by grants from the National Institute of General Medical Sciences (to K.S.R.). M.R.E. was supported by a postdoctoral fellowship from the American Cancer Society, and Z.M. was supported by a postdoctoral fellowship through the BioDefense Training grant (NIH).

Author Contributions D.P. performed and analysed most of the experiments in this study. A.C.T. performed Amnis ImageStream studies and the confocal microscopy analyses. M.R.E. helped with RT–PCR analyses and the *in vivo* mouse studies with BAI1-TSR. M.L. generated ELMO1 knockdown 774 cells. L.B.H. analysed the GEF activity associated with BAI1 and provided technical help in other parts of the manuscript. Z.M. performed the lipid membrane strip binding assay of the TSR protein. A.L.K. generated 2- μ m lipid vesicles. J.W.S. provided primary astrocytes, technical expertise and critical intellectual input with these studies. K.S.R. provided overall coordination with respect to conception, design and supervision of the study. K.S.R. also wrote the manuscript with comments from co-authors.

Author Information Reprints and permissions information is available at www.nature.com/reprints. Correspondence and requests for materials should be addressed to K.S.R. (ravi@virginia.edu).

METHODS

Cell culture and transfections. 293T cells and primary astrocytes were maintained in DMEM containing 10% FBS and 1% penicillin–streptomycin–glutamine⁵. LR73 Chinese hamster ovary cells, J774 macrophages and NIH 3T3 fibroblasts were cultured as described previously²⁰. Plasmid transfections into 293T cells were performed with calcium phosphate (Promega), and LR73 and NIH/3T3 cell transfections were performed with Lipofectamine 2000 (Invitrogen) in accordance with the manufacturer's instructions. Nucleofection was used to introduce plasmids and siRNA into J774 cells (Amaxa kit V, programme T-20) and primary astrocytes (Amaxa astrocyte kit, programme T-20).

Yeast two-hybrid screen. HF7C yeast strain (His⁻, Trp⁻, Leu⁻) was used to screen a mouse seven-day embryonic library²⁵ using pGBT10-N-term ELMO1 (residues 1–558) as bait. After screening of 1.1×10^7 colonies for growth on selective SCM plates (Trp⁻, Leu⁻, His⁻ with 5 mM 3-amino-1,2,4-triazole), and additional specificity/selection steps, the library plasmids were rescued and sequenced.

Plasmids and mutagenesis. ELMO, Dock180 and Rac constructs used in this study have been described previously^{5,14}. mBAl1, α -helix and non- α -helix constructs were generated by a PCR-based strategy from the yeast clone identified in the two-hybrid screen. Full-length pcDNA3.1(+)-BAl1 was a gift from T. Tokino. The various BAl1 constructs were generated by a PCR-based strategy. Flag and GFP sequence tags in the pEBB-BAl1–Flag and pEBB-BAl1–GFP constructs were inserted at the C-terminal end of BAl1; pEBB-HA–BAl1 construct was generated by inserting a tandem HA sequence tag near the N terminus, after the leader sequence (at the 50th amino-acid residue of BAl1). The pEBB-BAl1(without ECD)–Flag construct contained residues 1–50 fused to residues 951–1584, the pEBB-BAl1(without ICD)–Flag construct contained residues 1–1201, and the Flag–BAl1(ICD) construct contained residues 1192–1584. For bacterial production of GST–RGD–TSR, the sequence encoding residues 202–585 of BAl1 were introduced into the pGEX-4T2 vector. GST–RGD– Δ TSR contained residues 202–263 fused to residues 577–585 of BAl1. The RGD sequence of BAl1 (residues 231–233 of BAl1) was mutated to generate GST–RGE–TSR and GST–RGE– Δ TSR. All constructs were sequenced to confirm fidelity and the presence of the appropriate mutations.

Immunoprecipitation and immunoblotting. At 24–48 h after transfection of plasmids into 293T, LR73 or J774 cells, the cells were lysed and precipitated with the indicated antibodies or glutathione–Sepharose beads. Brain tissue was lysed and immunoprecipitated with anti-ELMO1 antibody conjugated with Protein A/G-agarose (Santa Cruz Biotechnology). Bound proteins were assessed by immunoblotting for the respective tags or endogenous proteins. The anti-ELMO1 antibody has been described previously⁵. The BAl1 antibody was obtained from Orbigen.

Immunofluorescence staining. NIH 3T3 or LR73 cells were plated on Labtek II slides and transfected with Lipofectamine 2000. At harvest, slides were washed with PBS, fixed in 3% formaldehyde and permeabilized with 0.2% Triton X-100. Cells were then blocked with clarified milk and subsequently stained with appropriate antibodies. Immunostaining was performed sequentially with IgG-specific secondary antibodies as described previously²⁰.

Quantitative RT–PCR. Total RNA from cell lines, tissues or primary cells was extracted with the use of an RNeasy Mini Kit (Qiagen) in accordance with the manufacturer's instructions. Complementary DNA was generated from 1.0 μ g of total RNA with Superscript III (Invitrogen) in accordance with the protocol. In all, 35 PCR cycles were performed for the amplification of mouse BAl1 with 1 μ l of the 20 μ l reaction mixture of cDNA.

Phagocytosis assay. LR73 or J774 cells were transiently transfected in triplicate with the indicated plasmids in a 24-well plate. At 24 h after transfection, engulfment assays were performed essentially as described previously²⁰, with either TAMRA-labelled apoptotic thymocytes or 2- μ m carboxylate-modified red fluorescent beads (Invitrogen) that mimic the negative charge on apoptotic cells and can serve as a simplified target^{12,19}. After being washed ten times with cold PBS, the cells were treated with trypsin, resuspended in cold medium (with 1% NaN₃) and analysed by two-colour flow cytometry. The transfected cells were recognized by their GFP fluorescence; targets (carboxylate-modified red fluorescent beads, apoptotic thymocytes or lipid vesicles) were recognized by red fluorescence. Forward and side-scatter parameters were used to distinguish unbound targets from cells. The data were analysed with FlowJo software.

Most double-positive cells scored in this flow-cytometry-based assay were targets engulfed by transfected cells or targets being engulfed, and not targets loosely bound to the cell surface (because these were removed during the extensive washing and trypsin treatment before flow cytometry).

The MFI in the red channel of the cells taking up targets gave an estimate of the efficiency of uptake (proportional to the number of particles taken up). To quantify the number of targets engulfed per cell, the images of the phagocytes as they were analysed by flow cytometry were obtained with Amnis ImageStream. Cell-surface staining of phagocytes for class I MHC expression was used to focus on the internalized targets and counting of targets was performed on a per-cell basis.

Red fluorescent microbubbles (2 μ m) containing phosphatidylcholine (100%) and phosphatidylserine (molar ratio of phosphatidylcholine to phosphatidylserine 85:15) were washed five times with PBS and resuspended with α -MEM supplemented with 2% FBS and 0.2% penicillin–streptomycin–glutamine. Vesicles (4×10^6) were added to each well of a 24-well plate; each well was then filled with the same medium. The 24-well plate was sealed, flipped over, and incubated at 37 °C for 2 h; the uptake was analysed by flow cytometry.

For *in vivo* analysis of BAl1 function, 10⁷ TAMRA-stained apoptotic thymocytes or 2 μ l of 2- μ m carboxylate beads (red labelled) were mixed with 3 μ g of GST or RGD–TSR proteins in 300 μ l of PBS. The 300 μ l mixtures of targets were injected into the peritoneum of either a wild-type or a LysM-Cre/YFP reporter mouse. At 20 min after injection, peritoneal exudate cells were collected. The cells were resuspended in 400 μ l of PBS containing 1% NaN₃. For wild-type C57Bl/6 mice that were used for the bead injections, to block Fc receptors, CD16/32 antibody was treated for 15 min and then the cells were stained with fluorescently labelled F4/80 antibody for 15 min. For LysM-Cre/YFP mice, the more than 98% YFP-positive cells in the peritoneum were F4/80-positive and CD11b-positive (and were CD3-negative and B220-negative). Either YFP-positive or F4/80-positive cells were gated to evaluate the fraction of macrophages ingesting red-labelled targets.

Binding assay of soluble TSRs. Jurkat cells (2.5×10^6) were washed with PBS and resuspended with 10 ml of X-Vivo10 medium in the 100-mm Petri dishes. The Jurkat cells were irradiated with ultraviolet and incubated at 37 °C for 2.5 h. The cells were washed twice with cold PBS and then resuspended in annexin V binding buffer containing 10 mM HEPES–NaOH pH 7.4, 140 mM NaCl, 2.5 mM CaCl₂ at a concentration of 10^5 cells ml⁻¹. Bacterially produced soluble TSR proteins (1 μ g) were incubated with 500 μ l of apoptotic Jurkat cell suspension for 15 min at room temperature (20 °C). After incubation, the cells were washed twice and resuspended with annexin V binding buffer. The presence of TSR proteins on apoptotic Jurkat cells was detected with anti-GST antibody (clone Z5; Santa Cruz) followed by Alexa 647-conjugated anti-IgG secondary antibody (Molecular Probes) and flow cytometry. The competitive binding of soluble TSRs with annexin V (Becton Dickinson) to 6- μ m carboxylate beads (Polysciences) or apoptotic Jurkat cells was performed as described above except that 1 μ g of the indicated proteins was incubated with the apoptotic Jurkat cells first for 15 min, followed by the addition of 5 μ l of FITC-conjugated annexin V for a further 15 min, and subsequent flow cytometry.

For inhibition assays, annexin V or the BAl1 recombinant fragments (10 ng μ l⁻¹) were added to 10⁷ apoptotic thymocytes and incubated for 15 min at room temperature. The mixture of proteins and apoptotic thymocytes was then added to J774 cells on a 24-well plate and analysed in the engulfment assay.

Binding of TSRs to lipids. The membrane lipid strips (Echelon Biosciences, Inc.) were blocked in 3% fatty-acid-free BSA in TBS-T containing 50 mM Tris–HCl pH 8.0, 150 mM NaCl and 0.1% Tween-20 for 1 h at room temperature in the dark. The membrane was then incubated at 4 °C with gentle agitation in the same solution containing the indicated purified proteins (each at 0.5 μ g ml⁻¹). The membranes were washed four times in TBS-T and then incubated for 1 h with anti-GST antibody (clone Z5; Santa Cruz) followed by routine immunoblotting steps.

CRIB pull-down assay. LR73 cells were transfected with BAl1 using Lipofectamine 2000. At 24 h after transfection, the cells were incubated with 2- μ m carboxylate beads for 30, 60 and 120 min. The cells were then washed with cold PBS twice and lysed. The cell lysates were incubated with 30 μ g of GST–CRIB for 1 h at 4 °C. The precipitation of Rac by GST–CRIB was detected by immunoblotting.